Journal of Applied Electrochemistry (2006) 36:179–186
DOI 10.1007/s10800-005-9052-4

Absorption/desorption of calcium ions on polypyrrole-loaded reticulated vitreous carbon

MAHMOUD M. SALEH[1], C. WEIDLICH[2], K.-M. MANGOLD[2] and K. JÜTTNER[2,*]
[1]*Chemistry Department, Faculty of Science, Cairo University, Cairo, Egypt*
[2]*Karl-Winnacker-Institute, DECHEMA e.V., Theodor-Heuss-Allee 25, D-60486, Frankfurt am Main, Germany*
*(*author for correspondence, e-mail: juettner@dechema.de)*

Received 31 January 2005; accepted in revised form 16 August 2005

Key words: absorption, calcium, cation exchange, polypyrrole, RVC

Abstract

Polypyrrole/polystyrene sulfonate-loaded reticulated vitreous carbon electrodes RVC/PPy/PSS were studied as electrochemical cation exchangers for the absorption of Ca^{2+} ions from aqueous solutions. Two grades of RVC were used mainly with 20 and 45 PPI. The preparation and characterization of the PPy/PSS layers on RVC are described. The structure and morphology of the porous electrodes were characterized using cyclic voltammetry (CV) and scanning electron microscopy (SEM). The potential dependent absorption and desorption of Ca^{2+} on RVC/PPy/PSS electrodes was studied in 0.1 M $CaCl_2$ solution using chronoamperometry and atomic adsorption spectroscopy (AAS). The extent of Ca^{2+} ions absorbed into RVC/PPy/PSS was found to increase with decreasing absorption potential, the specific surface area and the extent of polymer loading. Recovery of the RVC/PPy/PSS electrode was performed by anodic polarization at potentials at which Ca^{2+} ions are desorbed. The coulomb efficiency for the Ca^{2+} desorption process was found to be higher than that for the Ca^{2+} absorption process. From these results the feasibility of using RVC/PPy/PSS for water softening was determined under the prevailing experimental conditions.

1. Introduction

Conducting polymers have found many applications, such as for corrosion protection of metals [1–3], electrochromic devices [4], secondary batteries [5], anion/cation exchangers [6], and chemical and biochemical sensors [7]. The anion/cation exchange properties of conducting polymers have been studied extensively using different techniques [8–12]. These properties depend primarily on the type and size of the counterion incorporated into the polymer structure during its preparation [13–18]. For instance, polypyrrole PPy behaves as an anion exchanger if the chloride ion (Cl^-) is the counterion. This was attributed to the mobility of the Cl^- ion in the polymer film. If the counterions, such as polystyrene sulfonate (PSS^-) [16] or dodecyl benzene sulfonate (DBS^-) [8] are immobile, PPy behaves as a cation exchanger. However the ion exchange properties are found to be not only dependent on the counterion and the polymerization conditions but also on other factors, such as the electrolyte composition in the prevailing ion exchange process [19], the thickness of the polymer film [20], and the ageing of the polymer [21]. Although the number of fundamental studies in this area is high, less attention has been paid to applied studies.

In order to apply the principle of cation exchange to conducting polymers, the surface area of the substrate needs to be high. In this respect electropolymerisation of PPy onto the matrix of high surface area material, such as reticulated vitreous carbon (RVC), is not only of academic interest but also of practical importance. Several advantages of porous RVC electrodes have been reported. They include the high area/volume ratio, high porosity, conductivity, chemical and electrochemical stability, and machinability [22–24].

The present study aims to test the feasibility of RVC/PPy/PSS as a porous electrode structure for the removal of Ca^{2+} ions from drinking water under the conditions of stirred solutions. To demonstrate the principle of the ion exchange process on PPy/PSS, previous measurements on planar electrodes with an electrochemical quartz crystal microbalance (EQCM), will also be discussed [6, 16, 19].

2. Experimental

2.1. *Materials and chemicals*

The RVC blocks were kindly provided by ERG, Materials & Aerospace Corporation, AC. The pyrrole and other chemicals were obtained from Aldrich. The pyrrole monomer was distilled under nitrogen before use. The other chemicals were of pro analysis purity grade. The RVC electrodes had dimensions of $3.0 \times 4.0 \times 0.50$ cm^3. Two grades of RVC were available with 20 and 45 PPI, corresponding to specific areas of 14 and 30 cm^2 cm^{-3}, respectively. These are denoted here as RVC-20 and RVC-45. Electrical contact to the RVC blocks was made by Cu wire with silver epoxy resin coated with silicon rubber. These blocks are denoted as RVC electrodes in the following.

2.2. *Polymer preparation*

Polypyrrole was electrochemically prepared on RVC electrodes by electropolymerisation of pyrrole from aqueous solution of 0.2 M PPy + 0.2 M PSS. The electropolymerisation was carried out potentiostatically at E = +0.6 V vs. Ag/AgCl/KCl(sat.) reference electrode in a conventional three-electrode cell in stirred solution purged with N_2. To ensure uniform loading of polypyrrole into the porous substrate, two platinum sheets each of 1.5×2.0 cm^2 geometrical area were placed as counter-electrodes in the front and at the back of the RVC working electrode. The measured current densities referred to the geometrical areas (3×4 cm^2 = 12 cm^2) are 1.5 and 3.5 mA cm^{-2} for the RVC-20 and RVC-45, respectively. However, the actual current density referred to the inner surface area of the RVC cannot be calculated precisely because of the unknown potential and current distribution in the three-dimensional porous structure. The duration of electropolymerisation was 1 h for both RVC electrodes. Finally the electrodes were washed with de-ionized water and dried.

2.3. *Electrochemical measurements and Ca^{2+} absorption*

The electrochemical measurements were performed using a galvanostat/potentiostat, EG&G model 263 A. The EQCM was from ELCHEMA, model EQCN-501. The Ca^{2+} absorption/desorption experiments were carried out in the same cell used for the electropolymerisation of PPy on RVC. All measurements were performed in stirred aerated solution at room temperature. Absorption of Ca^{2+} ions into RVC/PPy/PSS from 0.1 M $CaCl_2$ was conducted at variable cathodic absorption potentials for a duration of 15 min. Subsequently the RVC electrodes were washed in pure water under stirring for 5 min and then rinsed thoroughly with water. The electrodes were then transferred into an electrochemical cell of 0.01 M NaCl where desorption experiments were carried out at fixed positive desorption potentials. After 15 min the NaCl solution was analyzed for calcium ions using atomic absorption spectroscopy (AAS), Perkin Elmer 1100B. The volume of the $CaCl_2$ and NaCl solutions was 150 ml.

3. Results and discussion

3.1. *Ion exchange behaviour of polypyrrole*

The ion exchange behaviour of PPy has been demonstrated by EQCM measurements [6, 19]. The scheme in Figure 1 illustrates the principle of the cation exchange process for PPy/PSS. The electrochemical oxidation and reduction of the conducting polymers is coupled with an exchange of ions with the outer solution to compensate the charge in the polymer. The immobility of the bulky PSS^- counterion causes exchange of cations to compensate the charge remaining in the polymer.

These cation exchanger properties are revealed by the simultaneous EQCM and CV measurements carried out in 0.1 M $CaCl_2$ solution [6, 16, 19]. In Figure 2 the mass of the polymer decreases on oxidation and increases on reduction, corresponding to the desorption and absorption of Ca^{2+} ions.

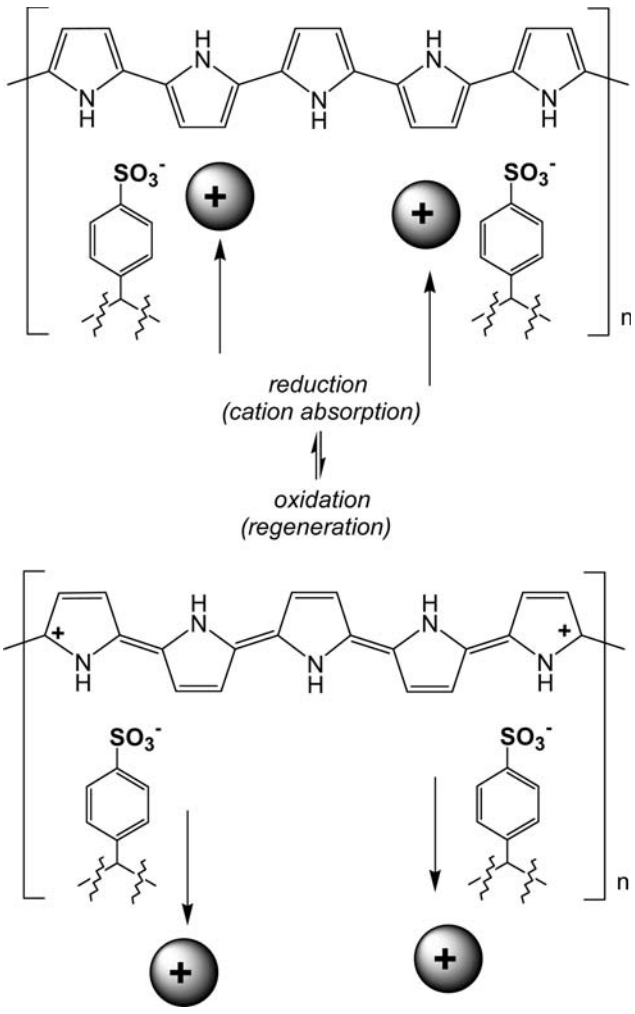

Fig. 1. Scheme of the absorption/desorption processes involved in reduction and oxidation of PPy/PSS.

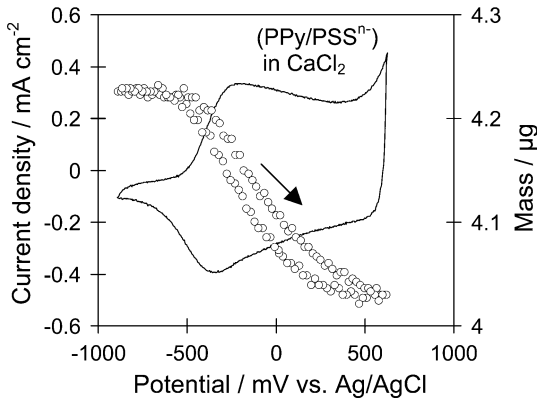

Fig. 2. EQCM mass (o) and cyclic voltammetric current (—) response of PPy/PSS^- in 0.1 M $CaCl_2$, v = 100 mV s^{-1}.

3.2. *Ion exchange behaviour of RVC/PPy/PSS*

3.2.1. *Electrode characterization*

As mentioned in the experimental section, the RVC/PPy/PSS electrodes were of two grades of porosity, namely 20 and 45 PPI. In the following the PPy/PSS loaded RVC electrodes will be denoted as RVC-20/PPy and RVC-45/PPy. SEM images of different RVC/PPy electrodes and bare RVC are shown in Figure 3a–c. The SEM images depict the porous structure of the RVC (Figure 3a) and the homogeneous surface of the bare RVC (Figure 3b) compared to a PPy/PSS covered RVC (Figure 3c). The morphology of the PPy/PSS layer in Figure 3c exhibits three-dimensional growth and is representative for the produced RVC/PPy/PSS electrodes. To figure out whether PPy was homogeneously deposited on RVC, images were also taken from the cross sections of these samples. These pictures exhibit PPy structures similar to that of Figure 3c indicating reasonable uniformity in the loading of PPy onto the RVC matrix. The total charge of electropolymerization obtained from the chronoamperometric curves on RVC-20 and RVC-45 was found to be 48 and 150 C, respectively. Assuming homogeneous distribution of PPy in the RVC matrix, which is reasonable from the SEM images, the charge density referring to the true inner surface area of RVC can be calculated from the specific surface area (14 and 30 cm^2 cm^{-3}) and the volume of the samples (6 cm^3) leading to 0.57 and 0.83 C cm^{-2} for RVC-20 and RVC-45, respectively.

Figure 4a and b shows cyclic voltammograms of Ca^{2+} absorption/desorption in 0.1 M $CaCl_2$ solution at different scan rates v = 5, 10, 20, 100 mV s^{-1} for RVC-20/PPy and RVC-45/PPy, respectively. The initial potential was −0.7 V. Two cycles were recorded but only the last one is presented here. The figures also include the CVs of the corresponding bare RVC electrodes. In both figures the broadening of the peaks in the CVs can be attributed to the influence of ohmic drop arising in such kinds of porous electrode structures. The currents on RVC-45/PPy are higher than those on RVC-20/PPy at the same potentials.

Another feature that is evident from Figure 4a is the levelling off of the current at potentials in the range of −0.3 to −0.7 V. This is prominent for the 20 PPI but not for the 45 PPI sample. The levelling off is also more pronounced at the lower scan rates of v = 5–20 mV s^{-1}. Active PPy loading is evident from the large difference in the CVs of bare RVC and RVC/PPy.

The number of monomer units in the PPy film can be estimated from the integral charge Q_a of the cyclic voltammograms if the degree of oxidation α_{ox} is known. For PPy the degree of oxidation α_{ox} = 0.25 is known from the literature [25]. This value means that one positive charge on the polymer chain is distributed over 4 monomer units. At v = 5 mV s^{-1} the anodic charges of the two samples were Q_a = 2.28 C and Q_a = 4.38 C

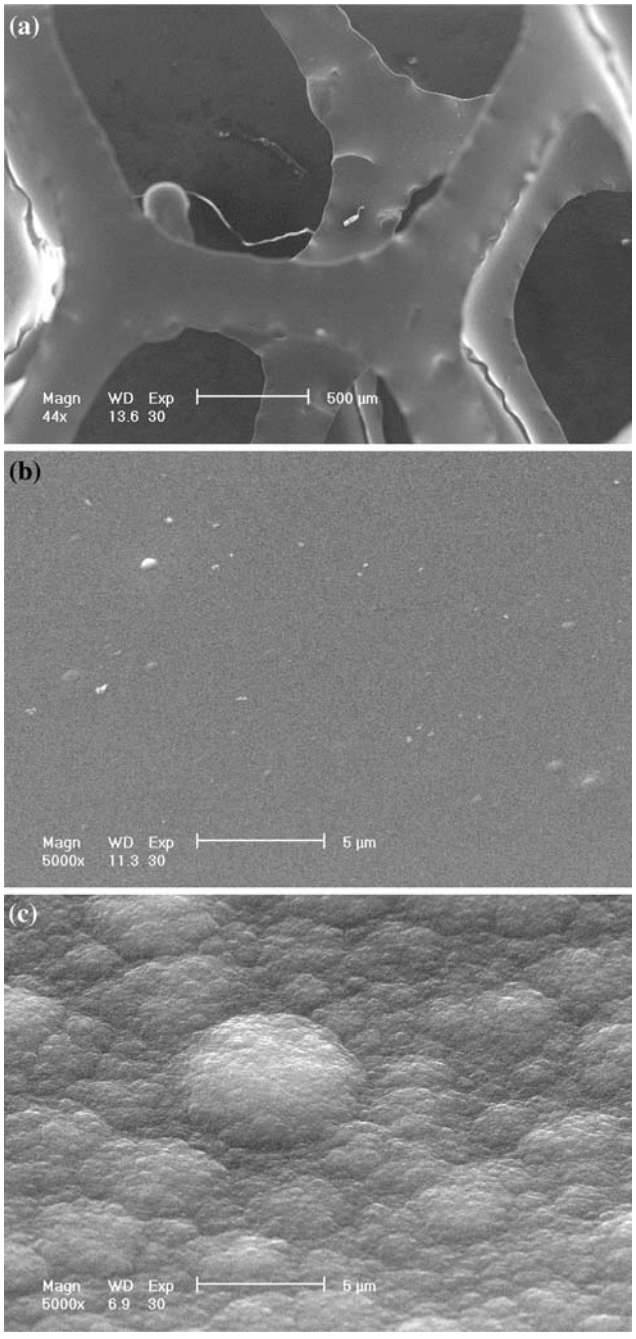

Fig. 3. SEM images of bare (a,b) and PPy/PSS covered (c) RVC-20.

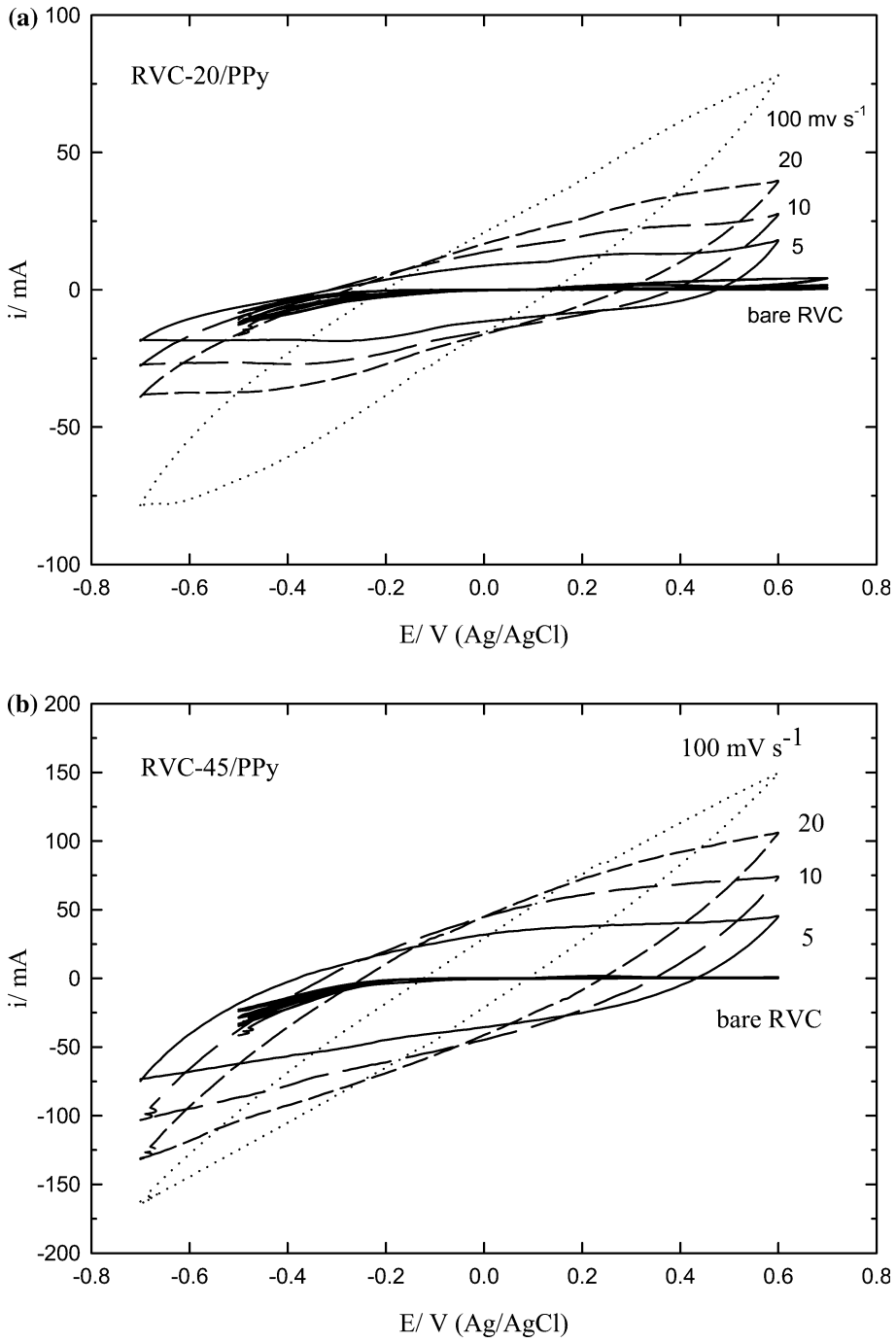

Fig. 4. Cyclic voltammograms of PPy-loaded RVC electrodes in 0.1 M $CaCl_2$ at different scan rates v = 5, 10, 20, 100 mV s^{-1}; (a) RVC-20/PPy, (b) RVC-45/PPy.

corresponding to 27 and 24 mC cm^{-2} per unit reaction area of RVC-20/PPy and RVC-45/PPy. From these data the amount of monomer units N_{mu}

$$N_{mu} = \frac{Q\mathrm{a}}{\alpha_{\mathrm{ox}} F} \qquad (1)$$

was calculated to be 1.125×10^{-6} mol cm^{-2} for RVC-20/PPy and 0.99×10^{-6} mol cm^{-2} for RVC-45/PPy.

3.2.2. *Calcium absorption/desorption*

The prepared electrodes RVC-20/PPy and RVC-45/PPy were used for Ca^{2+} absorption/desorption measurements. In these experiments the electrodes were polarized cathodically in 0.1 M $CaCl_2$ solution for 15 min to achieve Ca^{2+} absorption. After the washing procedure, described in the experimental part, the electrodes were polarized anodically for 15 min at fixed positive potentials in 0.01 M NaCl solution to achieve Ca^{2+} desorption. The Ca^{2+} concentrations measured after this process in 0.01 M NaCl solution were taken as a measure for the absorption extent of Ca^{2+} ions of the RVC/PPy/PSS electrodes. Figures 5 and 6 show the dependence of the Ca^{2+} concentration on the absorption potential for both electrodes. The desorption potentials in Figures 5

and 6 were fixed at $E_{des} = +0.4$ and $+0.5$ V, respectively. With decreasing absorption potential and/or increasing desorption potential the concentration of Ca^{2+} ions was found to increase for both electrodes. For RVC-20/PPy the increase in $[Ca^{2+}]$ at the desorption potential $E_{des} = +0.5$ V is not as significant as for $E_{des} = +0.4$ V. Furthermore, the $[Ca^{2+}]$ obtained on RVC-45/PPy is much higher than that on RVC-20/PPy under the same conditions. This could be due to the increase in surface area and/or the extent of loading PPy/PSS. It should be borne in mind that, in the case of RVC-45/PPy, the electropolymerization charge is about three times larger than that of RVC-20/PPy.

In practically every case a significant extent of absorption was only found at potentials $E_{abs} < -0.5$ V, as shown in Figures 5 and 6. However, it is not recommended to operate the electrodes at more negative potentials, i.e. $E_{abs} < -0.7$ V, where side reactions, such as hydrogen evolution or oxygen reduction, could be stimulated to a significant extent. It should be noted also that the differences in $[Ca^{2+}]$ at desorption potentials of $E_{des} = +0.5$ and $E_{des} = +0.4$ V for the same electrode are more significant in the absorption range $-0.5\ V < E_{abs} < -0.3$ V than at more negative potentials $E_{abs} < -0.5$ V. For instance, for RVC-45/PPy at $E_{abs} = -0.4$ V, the $[Ca^{2+}]$ at $E_{des} = +0.5$ V is about three times larger

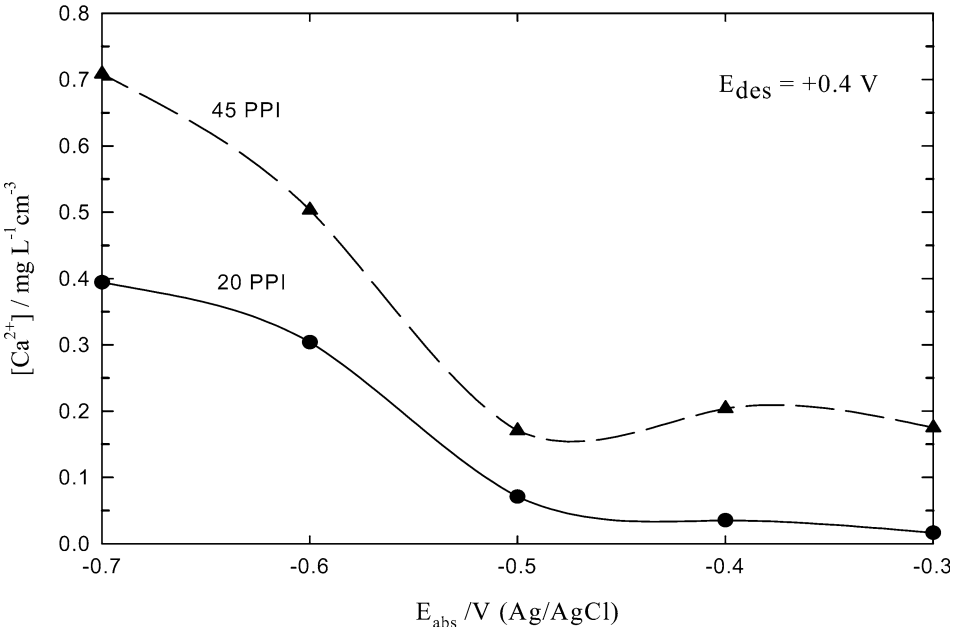

Fig. 5. Effect of absorption potential E_{abs} on $[Ca^{2+}]$ in 0.01 M NaCl solution for RVC-20/PPy and RVC-45/PPy electrodes at $E_{des} = +0.4$ V.

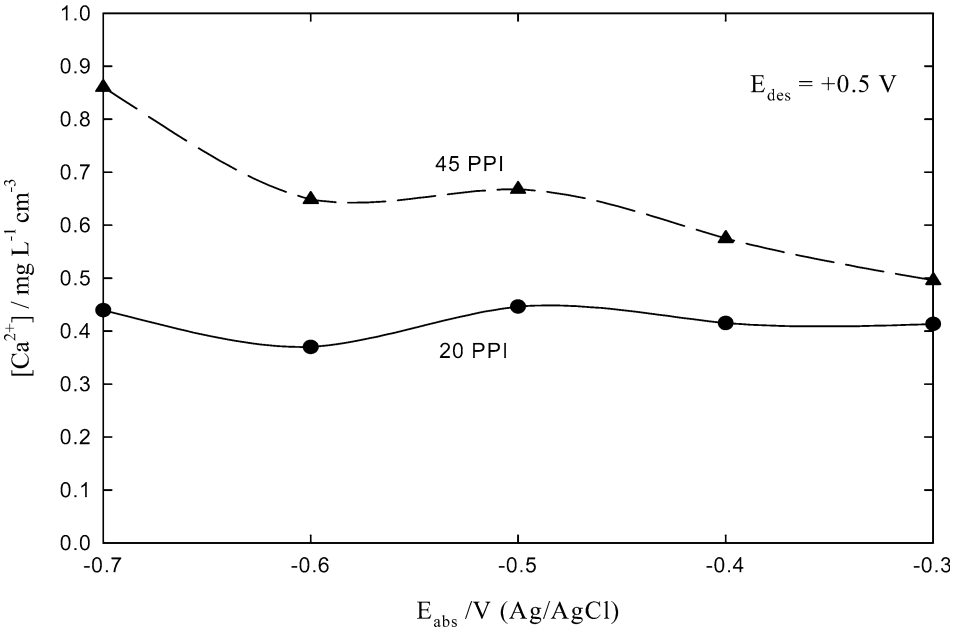

Fig. 6. Effect of absorption potential E_{abs} on $[Ca^{2+}]$ in 0.01 M NaCl solution for RVC-20/PPy and RVC-45/PPy electrodes at $E_{des} = +0.5$ V.

than that at $E_{des} = +0.4$ V. On the other hand, at $E_{abs} = -0.7$ V, the $[Ca^{2+}]$ at $E_{des} = +0.5$ V exceeds that at $E_{des} = +0.4$ V by about 1 mg l^{-1} only. The electrodes showed reasonable stability and the absorption/desorption cycles were repeated about 20 times without any evidence of losing efficiency. SEM images taken after the absorption-/desorption cycles showed no change in the polymer morphology.

3.3. *Coulomb efficiency*

The coulomb efficiency ζ for the absorption and desorption processes of Ca^{2+} on RVC/PPy/PSS electrodes is defined as:

$$\zeta = \frac{n_{Exp}}{n_{Th}} \times 100 \quad (2)$$

In Eq. (2) the experimental and theoretical mole numbers of calcium n_{Exp} and n_{Th} are obtained by absorption or desorption experiments. It should be noted that, although absorption and desorption efficiencies have the same expression, they differ in how n_{Exp} and n_{Th} are determined. The theoretical number n_{Th} was obtained from Faraday's law such that $n_{Th} = Q/z\mathrm{F}$, where Q is the total charge passed to obtain the specific extent of either absorption or desorption of Ca^{2+} ions and z is the number of charges transferred by absorption or desorption of one Ca^{2+}

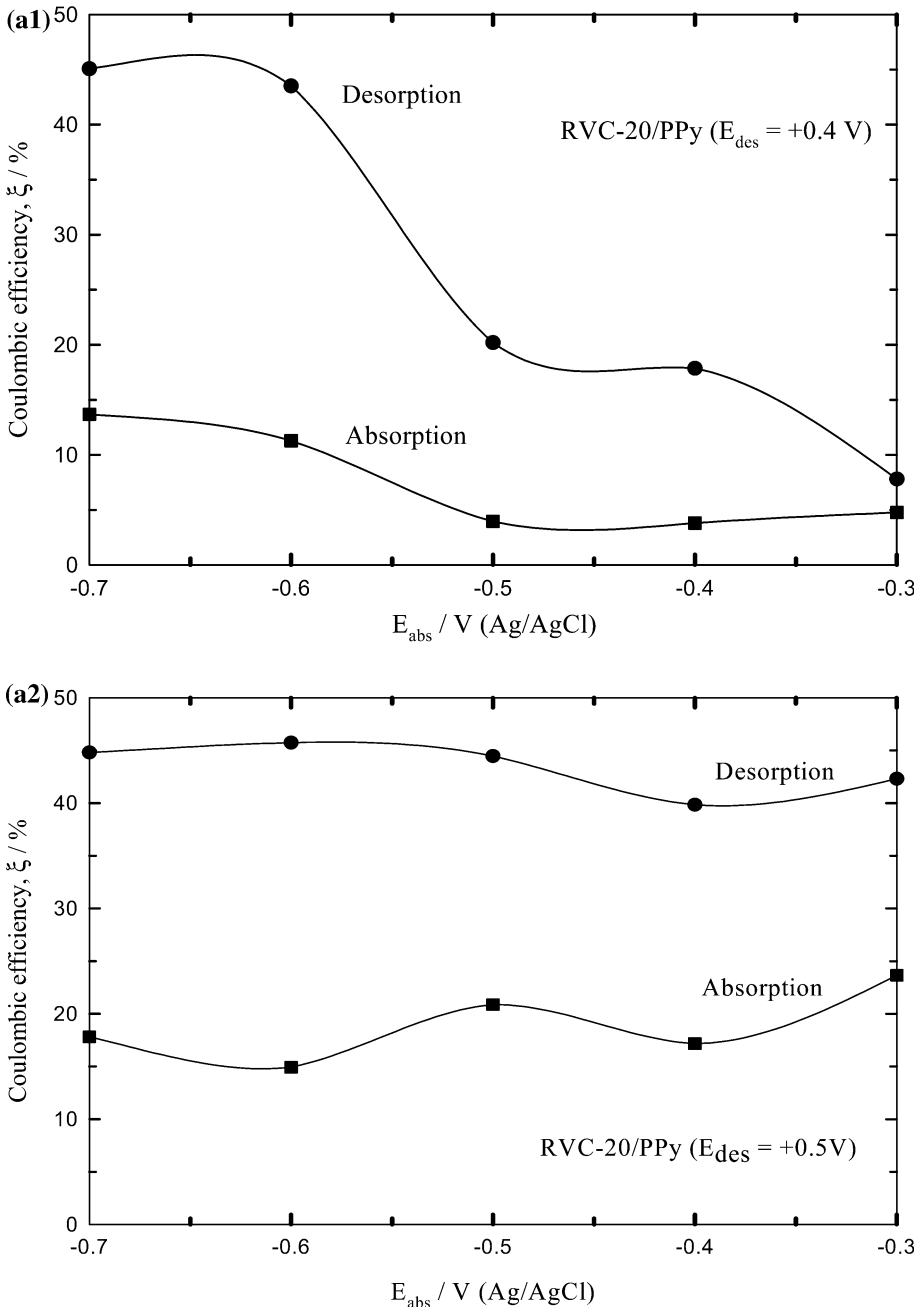

Fig. 7. Coulomb efficiency ζ for different electrodes RVC-20/PPy (a1, a2) and RVC-45/PPy (b1, b2), where index "1" corresponds to $E_{des} = +0.4$ V and index "2" to $E_{des} = +0.5$ V.

ion. The Q values were estimated from the area under the current transients associated with the absorption and desorption processes (not shown here). Since the transients for absorption and desorption differ from each other, two different Q values were obtained, one for absorption and one for desorption. The numbers n_{Exp} of moles Ca^{2+} were obtained from the AAS data shown in Figures 5 and 6 and used for the calculation of both ζ absorption and ζ desorption.

Figure 7a and b show the coulomb efficiency ζ for the Ca^{2+} absorption and desorption on RVC-20/PPy and RVC-45/PPy respectively. Generally, ζ increases as the absorption potential decreases and/or desorption potential increases. The values of the desorption efficiency are higher than those of the corresponding absorption efficiency for the same system parameters. The difference in the absorption and desorption efficiencies can be explained by a loss of Ca^{2+} during the washing procedure following the absorption process (see Experimental). Since the solution was not deaerated, an equivalent amount of Ca^{2+} may have been desorbed into the washing solution due to partial oxidation of PPy by dissolved O_2. This assumption has been proved by further experiments on a carbon electrode and will be published in a forthcoming paper [26].

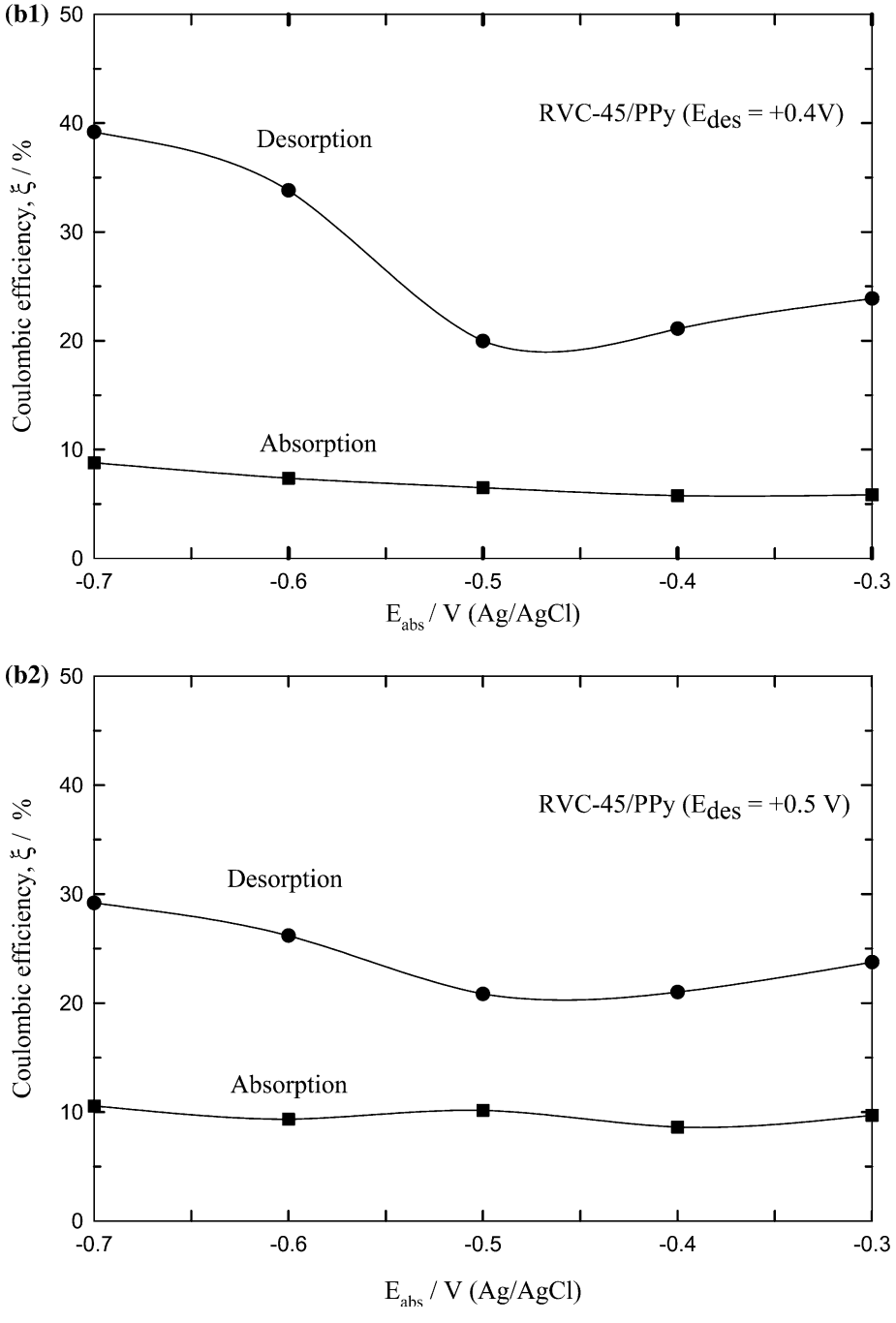

Fig. 7. (Continued)

The coulomb efficiency for RVC-20/PPy is higher than that for RVC-45/PPy. The values of ζ for absorption and desorption in the range of $-0.5\ \mathrm{V} < E_{abs} < -0.3\ \mathrm{V}$ are higher at $E_{des} = +0.5\ \mathrm{V}$ than that at $E_{des} = +0.4\ \mathrm{V}$. On the other hand, at $E_{abs} < -0.5\ \mathrm{V}$ the ζ values at $E_{des} = +0.5\ \mathrm{V}$ are comparable to those at $E_{des} = +0.4\ \mathrm{V}$. This is consistent with the results obtained in Figures 5 and 6. The overall coulomb efficiency is the net coulomb efficiency of both absorption and desorption processes.

4. Summary and conclusions

The absorption/desorption of Ca^{2+} ions on RVC/PPy/PSS electrodes was demonstrated by oxidation/reduction cycles in stirred solutions. This opens up potential applications of such materials for water softening with electrochemically controlled ion-exchangers. The removal of Ca^{2+} was found to depend on the absorption potential and the extent of polymer loading. Differences in the coulomb efficiency for absorption and desorption may be due to side reactions and other experimental shortcomings. For future developments it is of interest to use RVC/PPy electrodes in a flow-through regime to utilize a larger extent of the available reaction area and increased rates of mass transfer with porous electrodes.

References

1. T.D. Nguyen, M.C. Pham, B. Piro, J. Aubard, H. Takenouti and M. Keddam, *J. Electrochem. Soc.* **151** (2004) B 325.
2. U. Rammelt, P.T. Nguyen and W. Plieth, *Electrochim. Acta* **48** (2003) 1257.
3. N.V. Krstajic, B.N. Grgur, S.M. Jovanovic and M.V. Vojnovic, *Electrochim. Acta* **42** (1997) 1685.
4. M. Gazard, J.C. Dubois, M. Champagne, F. Garnier and G. Tourillon, *J. Phys. Colloque.* **44** (1983) c3–537.
5. P.J. Nigrey, D. MacInnes Jr, A.G. MacDiarmid and A.J. Heeger, *J. Electrochem. Soc.* **128** (1981) 1651.
6. C. Weidlich, K.-M. Mangold and K. Jüttner, *Electrochim. Acta* **47** (2001) 741.
7. N.C. Foulds and C.R. Lowe, *Anal. Chem.* **60** (1988) 2473.
8. V. Syriski, A. Opik and O. Forsen, *Electrochim. Acta* **48** (2003) 1409.
9. M. Hepel, *Electrochim. Acta* **41** (1996) 63.
10. M.A. Vorotyntsev, E. Vieil and J. Heinze, *J. Electroanal. Chem.* **450** (1998) 121.
11. S. Shimoda and E. Smela, *Electrochim. Acta* **44** (1998) 219.
12. X. Ren and P. Pickup, *Electrochim. Acta* **41** (1996) 1877.
13. K. Naoi, M. Lein and W.H. Smyrl, *J. Electroanal. Chem.* **272** (1989) 273.
14. K. Naoi, M. Lein and W.H. Smyrl, *J. Electrochem. Soc.* **138** (1991) 440.
15. T. Shimidzu, A. Ohtani and K. Honda, *J. Electroanal. Chem.* **251** (1988) 323.
16. C. Weidlich, K.-M. Mangold and K. Jüttner, *Syn. Met.* **119** (2001) 263.
17. M.A. Vorotyntsev, E. Vieil and J. Heinze, *Electrochim. Acta* **41** (1996) 1913.
18. X. Ren and P. Pickup, *J. Phys. Chem.* **97** (1993) 5356.
19. C. Weidlich, K.-M. Mangold and K. Jüttner, *Electrochim. Acta* **50** (2005) 1547.
20. G. Inzelt, V. Kertesz and A.S. Nyback, *J. Solid State Electrochem.* **3** (1999) 251.
21. C. Weidlich, K.-M. Mangold and K. Jüttner, *GDCh-Monographie* **18** (1999) 277.
22. J.M. Friedrich, C.G. Ponce-de-Leon, W. Reads and F.C. Walsh, *J. Electroanal. Chem.* **561** (2004) 203.
23. E.L. Gyenge and C.W. Oloman, *J. Appl. Electrochem.* **33** (2003) 665.
24. A. Alvarez–Gallegos and D. Pletcher, *Electrochim. Acta* **44** (1999) 2483.
25. K.K. Kanazawa, A.F. Diaz, W.D. Gill, P.M. Grant G.B. Street, *Synth. Met.* **1** (1979/80) 329.
26. K.-M. Mangold, C. Weidlich, J. Schuster and K. Jüttner, "Ion exchange properties and selectivity of PSS in an electrochemically switch able PPy matrix", *J. Appl. Electrochem.* (in print).